Desalination and Water Treatment 5 (2009) 80–90
www.deswater.com
1944-3994/1944-3986 © 2009 Desalination Publications. All rights reserved

Statistical design of experiments for dye-salt-water separation study using bimodal porous silica/γ-alumina membrane

A.L. Ahmad[a]*, C.P. Leo[b], S.R. Abd. Shukor[a]

[a]*School of Chemical Engineering, Engineering Campus, Universiti Sains Malaysia, Seri Ampangan, 14300 Nibong Tebal, S.P.S., Penang, Malaysia*
Tel.+604-5941012; Fax +604-5941013; email: chlatif@eng.usm.my
[b]*School of Engineering, Sunway Campus, Monash University, 46150 Bandar Sunway, Selangor, Malaysia*

Received 6 October 2008; Accepted 8 March 2009

ABSTRACT

Treatment of textile wastewater using conventional methods is either inefficient or costly. This is because it usually involves reactive dye, great amounts of salt and high temperature. In this study, a bimodal porous silica/γ-alumina membrane with improved permeability was tested in dye–salt water separation. The effects of temperature, feed concentration of dye, feed concentration of salt, pH and the pressure on permeate were examined using a response surface method. In general, the newly developed membrane showed satisfactory dye rejection (>90%) at common operating conditions. From the statistical analysis, it was found that the variation of salt rejection depends on the feed concentration of salt, feed concentration of dye and the pressure. Meanwhile, only the permeate flux is unaffected by the feed concentration of the dye.

Keywords: Dye; Salt; Membrane; Ceramic

1. Introduction

Textile wastewater is the most significant source of pollution in the industry due to its quantity and composition [1]. In the common dyeing process, an average of 70–150 L water, 0.6–0.8 kg NaCl and 30–60 g reactive dyes are used for 1 kg cotton [2]. The treatment bath containing more than 80% of the feed salt and 90% of the initial color is then discharged as wastewater. Treating such a great amount of effluent is a difficult task since conventional methods such as biological treatments, coagulation-flocculation, adsorption using activated carbon, electrochemical processes and ozone treatment have been found to be either costly or inefficient [2,3]. Consequently, textile wastewater treatment using membrane technology has been widely studied. Compared to other treatments, membrane separation not only shows high efficiency in color removal but also allows recycling of water and dyes for sustainable development in textile industry [3].

In general, membranes with different ranges of molecular weight cut-off (MWCO) can be utilized to achieve different treatment purposes in the textile industry. Microfiltration membranes and ultrafiltration membranes are useful for eliminating colloidal dyes, particles and marco-molecules; while nanofiltration (NF) membranes are applicable for removing reactive dyes [4]. Since reactive dyes are the major coloring agent in the textile industry [3], studies on reactive dye removal from textile effluent with high concentrations of salts using NF membranes

*Corresponding author.

Presented at EuroMed 2008, Desalination for Clean Water and Energy Cooperation among Mediterranean Countries of Europe and the MENA Region, 9–13 November 2008, King Hussein Bin Talal Convention Center, Dead Sea, Jordan.

have been greatly reported from two decades ago [5]. Many of these studies involved polyamide-based NF membranes with serious fouling [6–8]. As a result, recent studies have focused on low fouling membranes such as polysulfone NF membranes [3,9] and process optimization in order to reduce fouling [10,11]. Nevertheless, the use of polymeric membranes in textile wastewater treatment is still doubtful because it involves solutions with great variations of pH and high temperatures, which are less withstood by polymeric membranes. Different additives, e.g. peroxides, which are used to enhance the coloring process further, add weight to the durability of polymeric membranes [12].

Compared to polymeric membranes, ceramic membranes possess higher thermal stability and greater chemical resistance. For these reasons, ceramic membranes are more reliable and durable over polymeric membranes in the treatment of textile effluent [13]. In the separation of bromocresol green and salt, Guizard et al. [4] concluded that nanoporous ceramic membranes possess general behaviors assimilated to the characteristics of electrically charged organic NF membranes. Furthermore, Voigt et al. [14] have successfully utilized titania ceramic membranes in cleaning colored wastewater from the textile finishing. High color removal (70–100%) was achieved with a desalting of 10–59%, depending on the wastewater composition. In addition, the application of ceramic membranes in NF is no longer limited by the low permeability as in the past. Several researchers have tailored ceramic membranes with favorable asymmetric porous structure to achieve high permeability [15–18]. Our previous study even showed that bimodal porous γ-alumina layer can be used to improve the permeability of silica/γ-alumina membrane in dye separation and salt separation [19].

Further study of dye–salt water separation using this bimodal porous ceramic membrane is definitely required to fully understand its separation characteristics. This study is also important to predict future application of this newly developed membrane in textile wastewater treatment because the information leads to the module selection and separation system design efficiently.

For these reasons, the design of experiments (DOE) is performed to investigate the effects of common operating conditions on the quality and quantity of permeate when a bimodal porous silica/γ-alumina membrane was used to a separate dye–salt water mixture containing reactive dye (RR120, MW = 1469.98 Da) and NaCl. DOE adopts both mathematical and statistical techniques for modeling and analysis of problems in which responses of interest are influenced by several variables. For a large number of variables, the response surface method (RSM) is chosen because it allows fractionally factorial search of response model by examining simultaneous, systematic and efficient variation of important components [20]. A simple linear model and quadratic models are used to represent the significant effect of the operational conditions on the interested responses. It is of course unlikely that a polynomial model will be a reasonable approximation of the true functional relationship over the entire space of the independent variable. However, they usually work well for a relatively small region [20]. The eventual objective of this study is to learn the effect of common operational conditions on the permeate quantity and quality of the newly developed membrane which is difficult to be fully understood via one-factor-at-a-time strategy.

In this study, the separation of dye–salt water mixtures is carried out using a bimodal porous silica/γ-alumina membrane with improved permeability. The RSM with central composite design (CCD) is performed to study influences of common operating conditions on the quality and quantity of permeate. The CCD is composed of five factors: temperature (25–50 °C), feed concentration of dye (1–3 g/L), feed concentration of salt (20–80 g/L), pH (pH 5–9) and pressure (5–10 bar). The responses which are of interest in this study are the percentage retention of dye, the percentage retention of salt, and the permeate flux. Polynomial models are used to represent the significant effects of the operational conditions on the interested responses. Besides that, it is of interest to determine optimum conditions for achieving a high rejection of dye, maximum desalting and large permeate flux.

2. Experimental procedure

The preparation method of silica/γ-alumina membranes with a bimodal porous intermediate layer via sol-gel routes has been reported in previous works [21,22]. Silica sol was synthesized using the method introduced by Honma et al. [23] while boehmite sol was prepared as described by Lambert et al. [24]. Besides that, polystyrene beads were added into the boehmite sol for creating secondary pores (diameter ca. 50 nm) in the γ-alumina layer which greatly enhances membrane permeability. Fig. 1 shows the schematic of the bimodal porous silica/γ-alumina membrane with TEM pictures of the silica and bimodal porous γ-alumina layers. As reported before [19], the membrane permeability is improved to 0.22×10^{-12} m, but the MWCO of the membrane is maintained at 400 Da. The improved silica/γ-alumina membrane can be categorized as a NF membrane since MWCO was controlled within the range of 300–500 Da.

In this work, the bimodal porous silica/γ-alumina membrane was further tested in dye–salt water separation using a dead-end permeation set-up as shown in Fig. 2. The feed solution contained 1–3 g/L Reactive Red 120 (MW = 1469.98 Da, Sigma-Aldrich) and 20–80 g/L NaCl (Merck). The solution pH was adjusted using either 0.01 M HCl solution or 0.01 M NaOH solution. In addition, the

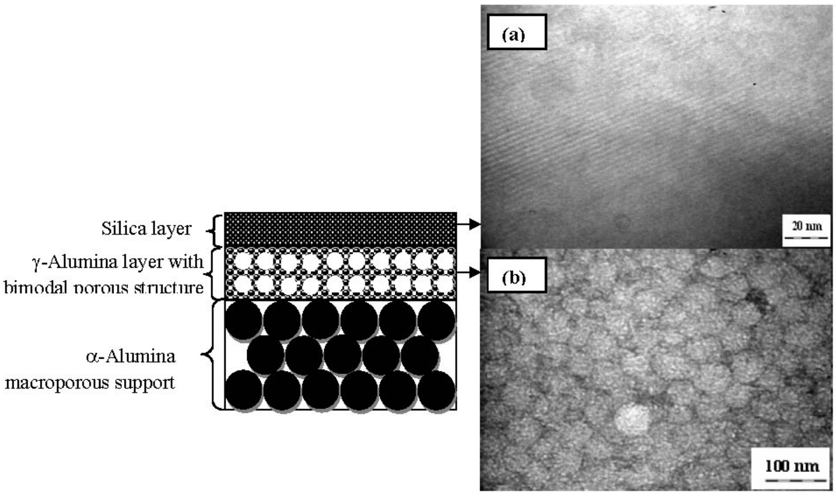

Fig. 1. Schematic of silica/γ-alumina membrane with (a) TEM picture of silica layer and (b) TEM picture of bimodal porous γ-alumina layer

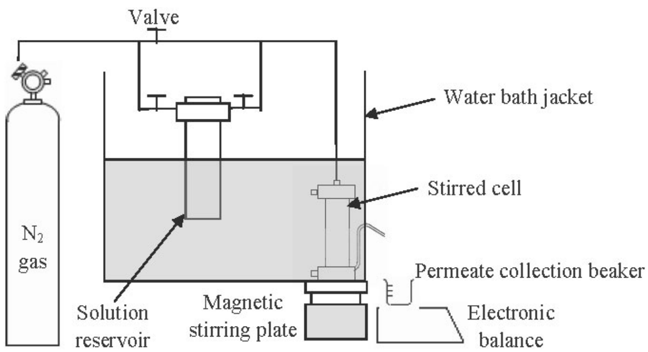

Fig. 2. Schematic of the experimental rig for liquid permeation test.

temperature was controlled in the range of 25–50 °C using a water bath while the pressure was controlled in the range of 5–10 bar using a regulator. The concentration of the RR120 in permeate samples was then measured using a UV-Vis spectrophotometer (Thermo Spectronic, USA; model GENESYS 2) at 530 nm. The NaCl content in the permeate samples from the dye–salt water separation runs was determined using an inductive coupled plasma-emission spectrophotomer (Optima 3000, Perkin Elmer) with dilution. The last response, permeate flux (J_w, L.m^{-2}.h^{-1}) was calculated using Eq. (1).

$$J_w = \frac{(w_2 - w_1)}{\rho A t} \quad (1)$$

where w_1 is the initial weight of permeate, g; w_2 the final weight of permeate, g; ρ the density of permeate, g/cm^3; A the surface area of membrane for filtration, m^2; and t the duration for permeate collection, h. Instead of using one-factor-at-a-time experiments, DOE was used to study the effects of common operating conditions on the permeate quality and the permeate quantity when a bimodal porous silica/γ-alumina membrane was utilized. In this study, RSM with CCD was performed (Table 1). In Table 1, it is seen that CCD is composed of five factors: temperature (A), feed concentration of dye (B), feed concentration of salt (C), pH (D) and pressure (E). The ranges of factors were selected based on the literature [2], and they are common operating conditions for textile wastewater treatment. Responses which are of interest in this study are the percentage retention of dye (Y_1), the percentage retention of salt (Y_2), and the permeate flux (Y_3). For the five factors, half-fractional DOE was chosen to avoid excessive runs of experiments. Each numeric factor was only varied over five levels: plus and minus alpha (axial points), plus and minus 1 (factorial points) and the center point. Table 2 shows the experiments with three center points which were statistically chosen using Design Expert software. The regression models were generated for further optimization study. In dye–salt water separation, it was desired to achieve maximum separation of dye, minimum salt rejection and high permeate flux. Table 3 shows the goal of each factor and responses. For multiple responses, the constrained optimization problem was solved using nonlinear programming method available in Design Expert software.

Table 1
Experimental conditions of dye–salt water separation

Factor	Code	Low actual	High actual	Low coded	High coded
Temperature, °C	A	25	50	−1	1
$C_{F,\text{dye}}{}^{a}$, g/L	B	1	3	−1	1
$C_{F,\text{salt}}{}^{b}$, g/L	C	20	80	−1	1
pH	D	7	9	−1	1
Pressure, bar	E	5	10	−1	1

[a]Feed concentration of dye.
[b]Feed concentration of salt.

Table 2
CCD arrangement and responses for NF of dye and salt mixture in aqueous solution

Run	Factor					Response		
	A	B	C	D	E	Y_1	Y_2	Y_3
	Temperature (°C)	$C_{F,\,dye}$[a] (g/L)	$C_{F,salt}$[b] (g/L)	pH	Pressure (bar)	R_{dye}[c] (%)	R_{salt}[d] (%)	Flux ($L.m^{-2}.h^{-1}$)
1	25.0	1	80	5	5.0	91.43	11.73	3.72
2	25.0	3	20	5	5.0	94.69	16.32	3.82
3	25.0	3	20	9	10.0	97.89	60.45	7.45
4	25.0	1	80	9	10.0	94.11	29.81	5.45
5	37.5	2	50	7	7.5	94.87	44.32	6.57
6	25.0	3	80	5	10.0	98.15	27.88	6.45
7	50.0	3	20	5	10.0	98.88	58.23	13.88
8	37.5	1	50	7	7.5	92.88	45.28	7.10
9	25.0	2	50	7	7.5	95.12	42.78	4.89
10	50.0	3	80	9	10.0	98.22	26.34	12.15
11	50.0	1	80	9	5.0	91.45	12.34	6.35
12	25.0	3	80	9	5.0	94.68	10.93	3.65
13	50.0	1	20	5	5.0	91.45	20.38	7.26
14	37.5	2	50	7	7.5	93.95	43.26	6.66
15	50.0	3	20	9	5.0	95.75	16.45	6.85
16	37.5	2	50	5	7.5	95.36	43.76	6.63
17	37.5	2	50	7	7.5	94.75	44.01	6.82
18	37.5	3	50	7	7.5	97.27	39.87	6.83
19	25.0	1	20	5	10.0	94.12	64.23	7.98
20	37.5	2	80	7	7.5	94.67	25.73	5.56
21	37.5	2	50	7	5.0	93.65	14.75	5.78
22	50.0	1	20	9	10.0	94.23	65.23	13.34
23	25.0	1	20	9	5.0	91.20	19.76	3.88
24	50.0	3	80	5	5.0	95.46	10.93	6.30
25	37.5	2	50	7	10.0	95.44	43.65	10.34
26	50.0	2	50	7	7.5	94.65	44.25	9.12
27	37.5	2	50	9	7.5	94.07	40.63	6.72
28	37.5	2	20	7	7.5	94.32	48.75	6.89
29	50.0	1	80	5	10.0	93.89	29.38	12.03

[a]Feed concentration of dye. [b]Feed concentration of salt. [c]Retention of dye. [d]Retention of salt.

Table 3
Constraints for optimum operation conditions of dye–salt water separation

Variables	Goal	Lower limit	Upper limit	Lower weight	Upper weight	Importance
Temperature (°C)	Within range	25	50	1	1	3
$C_{F,dye}$[a] (g/L)	Within range	1	3	1	1	3
$C_{F,salt}$[b] (g/L)	Within range	20	80	1	1	3
pH	Within range	5	9	1	1	3
Pressure (bar)	Within range	5	10	1	1	3
R_{dye}[c] (%)	Maximize	91.2	98.88	1	1	1
R_{salt}[d] (%)	Minimize	10.93	65.23	1	1	3
Flux ($L.m^{-2}.h^{-1}$)	Maximize	3.65	13.88	1	1	3

[a]Feed concentration of dye. [b]Feed concentration of salt. [c]Retention of dye. [d]Retention of salt.

3. Results and discussion

3.1. Effect of process variables on dye rejection

The rejection of dye achieves more than 90% for different types of operating conditions and feed concentrations as shown in Table 2. This is possibly because the retention is strongly controlled by a sieving mechanism when the molecular weight of the dye (RR120, MW = 1469.98 Da) is higher than the membrane MWCO (400 Da) and [7]. However, the percentage of decolorization varies slightly with the test conditions, in the range of 91–99% as shown in Table 2. The lowest dye rejection is observed in Run 23 and the highest dye rejection is observed in Run 7. Without performing statistical analysis, a precise conclusion of the observation is difficult to be made.

In the statistical analysis, a linear model is chosen to represent the effects of common operating conditions on the dye rejection. The insignificant terms such as temperature, feed concentration of salt and pH are further removed from the linear model. The ANOVA results of the reduced model are summarized in Table 4. ANOVA results show that the reduced linear model for dye rejection is significant in the F test and insignificant in the lack of fit. Both calculations confirm that it is acceptable from the statistical point of view to represent the experimental data of dye rejection using this reduced linear model. In addition, there were works in literatures which reported that dye rejection is unaffected by temperature [25], addition of salt [26] and pH of feed solutions [27] in the NF of aqueous solution with salt and large dye molecules (>1000 Da) . Thus, it is reasonable to have only feed concentration of dye (B) and operating pressure (E) as the factors in the chosen model. The feed concentration of dye (B) and the operating pressure (E) are significant at 99.99% confidence level as they present a probability lower than 0.0001. Comparing the feed concentration of dye (B) and the operating pressure (E), the latter factor has a lower effect on the dye rejection since it only contributes 31.27% of the total variance.

From Table 4, R^2 of the selected model at 96.04% is quite satisfactory. R^2, which is adjusted for the number of terms in the model, is also acceptable as the reduced model will be expected to explain about 95.73% of the variability in new data using two factors. In addition, the predicted R^2 of the reduced model (95.18%) is close to the adjusted R^2 (95.73%). There is no outlier in the data as the difference is less than 20%. In conclusion, the reduced linear model is adequate for the observed dye rejection.

The equations to represent the model in terms of coded factors [Eq. (2)] and in terms of actual factors [Eq. (3)] are generated and shown as below:

$$R_{\text{dye}} = 94.71 + 2.0B + 1.40E \tag{2}$$

$$R_{\text{dye}} = 86.48963 + 2.01278\,C_{\text{dye}} + 0.55933\ \text{pressure} \tag{3}$$

From Eqs. (2) and (3), the coefficient of each factor represents the effect of the corresponding factor on the dye retention. It is observed that the dye retention is synergistically affected by the operating pressure and the feed concentration of dye. However, the two factors affect dye rejection independently as the interaction term is absent in the equations. In addition, the experimental results can be interpreted from the contour plot [Fig. 3 (a)] and the 3-D plot [Fig. 3 (b)] of response surfaces. The contours are parallel straight lines and the 3-D plot is a plane because the model is first order with only the main effect of factor B (feed concentration of dye) and factor E (pressure) present. The plots also suggest that the dye retention is high if the pressure and the feed concentration of dye are at high levels. Thus, better color removal is expected to be achieved at higher feed concentration of dye in the dye–salt water mixture as reported by Al-Aseeri et al. [26]. Besides that, the model concludes that the dye rejection increases slightly with operating pressure which is analogous with the finding of other works [25,26]. The observation in this section cannot be explained by the

Table 4
ANOVA result of response surface reduced linear model for dye rejection

Source	Sum of squares	DF[a]	Mean square	F[b] value	Probability >F	Remarks
Model	108.12	2	54.06	315.63	<0.0001	Significant
B	72.92	1	72.92	425.76	<0.0001	
E	35.20	1	35.20	205.49	<0.0001	
Residual	4.45	26	0.17			
Lack of fit	3.95	24	0.16	0.66	0.7609	Not significant
Pure error	0.50	2	0.25			
Corrected total	112.57	28				

R^2 = 0.9604   Adjusted R^2 = 0.9573   Predicted R^2 = 0.9518

[a]Degrees of freedom; [b]Fisher.

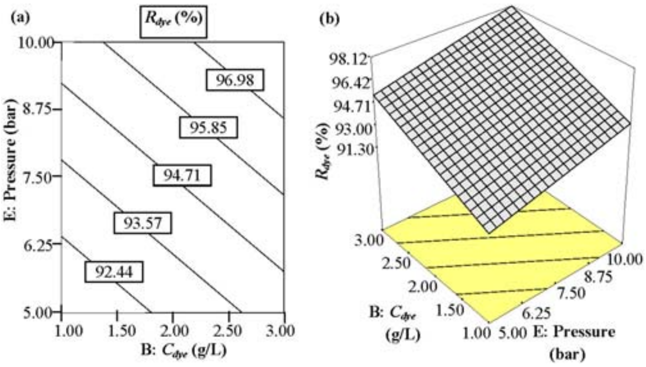

Fig. 3. (a) Contour plot and (b) surface response plot for effect of pressure and feed concentration of dye on dye rejection.

usual polarization phenomenon which causes the retention of small solutes to be lower at higher pressure and feed concentration [27,28]. Retention can be higher in the case of macromolecular solutes mixture when concentration polarization can have a strong influence on the selectivity [28]. It is obvious that concentration polarization promotes retention of RR120 due to the high selectivity of dye molecules compared to salt.

3.2. Effect of process variables on salt rejection

Using bimodal porous silica/γ-alumina membrane, a great variation of salt retention is observed in dye–salt water separation as shown in Table 2. The salt retention varies from 11% to 65% depending on the experimental conditions. This is because salt rejection by silica/γ-alumina membranes is strongly based on electrostatic interactions between the ions in solution and the charged pores of the membrane [29]. Without much sieving effect, the percentage of salt rejection is subjected to the separation variables. From Table 2, it can be deduced that the pressure (factor E) and the feed concentration of salt (factor C) affect the rejection of salt. However, the significance of other factors such as dye feed concentration, pH and temperature are undetermined by looking at Table 2.

In this section, a quadratic model is recommended for the observed salt retention. However, there are only few factors that should be included in the quadratic model as shown in the ANOVA results of the reduced quadratic model (Table 5). The significant terms include the main effect of dye feed concentration (B), salt feed concentration (C) and pressure (E); quadratic effect of salt feed concentration (C^2) and pressure (E^2); as well as interaction effect of salt feed concentration and pressure (CE). These terms show probability smaller than 0.05 for rejection of the null hypothesis. The salt retention is most influenced by factor C (pressure) as this factor contributes 56.83% of the total variances. Compared to factor C (pressure) and E (feed concentration of salt), factor B (feed concentration of dye) gives the smallest effect on the salt retention. Besides that, the ANOVA results in Table 5 indicate that the model fits the observation well. This is because the fitted second-order response surface model is highly significant with an F-test value of 205.59 and insignificant in the lack of fit test. Also, the reduced quadratic model possesses high R^2 (0.9910), which signifies that the predicted salt retention values are close to the observed salt retention values. Furthermore, the adjusted R^2 and predicted R^2 for the reduced quadratic model are 0.9886 and 0.9822 respectively. A difference below 0.20 for these values shows the absence of outliers and the adequacy of the model.

The coefficients of each term are calculated to form the equations for the salt retention prediction. The formula is written in coded terms [Eq. (4)] and actual terms [Eq. (5)]. However, it is difficult to determine whether the factor is giving synergistic or antagonistic effect on salt retention. The equations not only involve quadratic terms of some factors but also an interaction term of salt feed concentration and pressure.

$$R_{\mathrm{NaCl}} = 42.49 - 1.71\mathrm{B} - 10.26C + 15.09\times10^{-2.396}\,C^2 - 10.43\,E^2 - 6.73\,CE \tag{4}$$

$$\begin{aligned} R_{\mathrm{NaCl}} = {} & -116.47760 - 1.70736\,C_{F,\mathrm{dye}} + 0.59731\,C_{F,\mathrm{NaCl}} \\ & + 35.56542\,(\text{pressure}) - 2.65911\times10^{-3}\,(C_{F,\mathrm{NaCl}})^2 \\ & - 1.66931\,(\text{pressure})^2 - 0.089798\,(C_{F,\mathrm{NaCl}})\,(\text{pressure}) \end{aligned} \tag{5}$$

Compared to these equations, the perturbation plot for salt retention (Fig. 4) shows a better picture of the term effect. The perturbation plot is helpful in comparing the effect of all the factors at a particular point in the design space. The response is plotted by changing only one factor over its range while holding of the other factors constant. By default, the reference point in the graph is at the midpoint (coded 0) of all the factors.

As shown in Fig. 4, steep slopes are found in factor E (pressure) and C (feed concentration of salt). This observation shows that the salt retention is sensitive to the changes of pressure and salt feed concentration. A relatively flat line in factor B (feed concentration of dye) shows insensitivity of salt removal to the change in dye feed concentration. From Fig. 4, it is seen that the feed concentration of dye and salt give antagonistic effect on the salt retention while the pressure gives a synergistic effect on the salt retention. However, the plot is like “one factor at a time” experimentation and does not show the effect of interactions.

The antagonistic effect of salt concentration on the salt retention percentage can be related to the principle of

Table 5
ANOVA result of response surface reduced quadratic model for salt rejection

Source	Sum of squares	DF[a]	Mean square	F[b] value	Probability >F	Remarks
Model	7795.89	6	1299.31	205.59	<0.0001	Significant
B	52.47	1	52.47	16.38	0.0005	
C	1895.79	1	1895.79	591.78	<0.0001	
E	4098.52	1	4098.52	1279.38	<0.0001	
C^2	19.55	1	19.55	6.10	0.0217	
E^2	371.64	1	371.64	116.01	<0.0001	
CE	725.73	1	725.73	226.54	<0.0001	
Residual	70.48	22	3.20			
Lack of fit	69.88	20	3.49	11.76	0.0812	Not significant
Pure error	0.59	2	0.30			
Corrected total	7866.37	28				
R^2 = 0.991	Adjusted R^2 = 0.9886;		Predicted R^2 = 0.9822			

[a]Degrees of freedom; [b]Fisher.

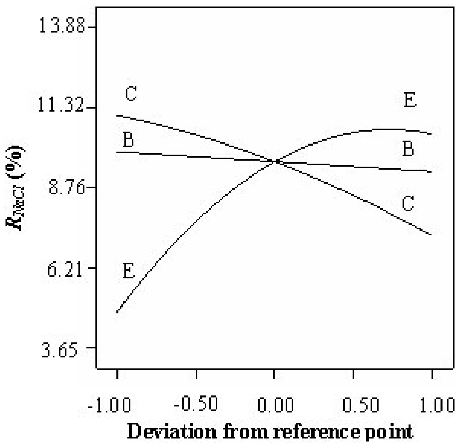

Fig. 4. Perturbation plot for permeate flux.

Donnan equilibrium. Repulsive force of the ceramic membrane (negatively charged) decreases with increasing salt concentration due to higher concentrations of Na^+ cations on the membrane surface. Overcoming the repulsive force also allows more Cl^- anions to pass through the membrane. More salt permeate through the ceramic membrane at higher NaCl feed concentration, and this lowers the salt rejection [6]. Specifically, the reduction in salt retention is possibly due to the concentration polarization phenomenon. For aqueous solution with high concentration of salt and dye, the effect of concentration polarization is unavoidable in NF. Due to the increased solute concentration at the membrane surface, the observed retention will be lower than the real retention. Thus, increasing the concentration of salt and dye in the feed solution results a lower salt retention. The range of dye feed concentration (1–3 g/L) is far lower than salt feed concentration (20–80 g/L) in the design space. Consequently, the main effect of the dye feed concen-tration on the salt retention is less significant compared to the feed concentration of salt.

It is noted that the salt rejection improved with increasing flux because the chloride salts retention is enhanced by convection mechanism as flux increases [30]. Pressure is one of the main driving forces for flux so it is reasonable to have positive main effect of pressure on the salt retention. The synergetic effect of pressure on the salt retention, however, is limited by the quadratic effect of pressure. At higher flux, the rejection of salt decreases slightly due to more severe concentration polarization. Besides that, the interaction term of pressure and the feed concentration of salt can be explained by the occurrence of osmotic pressure. Osmotic pressure depends on the difference of salt concentration over the membrane [8]. The osmotic pressure increases with the salt feed concentration and it results in a lower rejection of salt.

Contour plot and surface response plot (Fig. 5) show the effect of two factors, pressure and feed concentration of salt, when the feed concentration of dye is 2 g/L. As observed from Fig. 5, a combination of high pressure and low salt feed concentration leads to great rejection of salt. The operating pressure should be set higher than 7.5 bar if salt retention higher than 50% is desired. The effect of dye feed concentration on the salt retention is illustrated in Fig. 6. From Fig. 6, it is obvious that the salt retention is strongly affected by pressure compared to dye feed concentration. This is because variation of salt retention is small even there are changes of dye concentration for pressure higher than 7.5 bar. In conclusion, high salt retention can be achieved at low feed concentration of salt and high pressure.

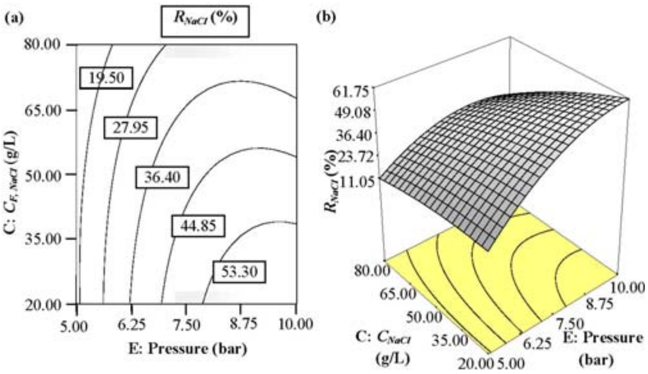

Fig. 5. (a) Contour plot and (b) surface response plot for effect of pressure and feed concentration of salt on salt rejection (C_{dye} = 2 g/L).

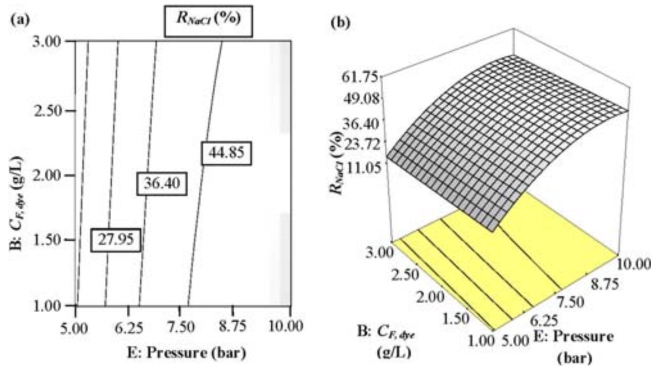

Fig. 6. (a) Contour plot and (b) surface response plot for effect of pressure and feed concentration of dye on salt rejection ($C_{F,\mathrm{NaCl}}$ = 50 g/L).

Table 6
ANOVA result of response surface final quadratic model for permeate flux

Source	Sum of squares	DF[a]	Mean square	F[b] value	Probability >F	Remarks
Model	207.30	8	25.91	453.37	<0.0001	Significant
A	88.83	1	88.83	1554.20	<0.0001	
C	5.23	1	5.23	91.46	<0.0001	
D	0.28	1	0.28	4.82	0.0401	
E	95.53	1	95.53	1671.42	<0.0001	
C^2	1.06	1	1.06	18.57	0.0003	
E^2	5.58	1	5.59	97.79	<0.0001	
AE	9.60	1	9.60	167.91	<0.0001	
CE	1.43	1	1.43	24.96	<0.0001	
Residual	1.14	20	0.06			
Lack of fit	1.11	18	0.06	3.85	0.2259	Not significant
Pure error	0.03	2	0.01			
Corrected total	208.44	28				

R^2 = 0.9945; Adjusted R^2 = 0.9871; Predicted R^2 = 0.9923

[a]Degree of freedom; [b]Fisher.

3.3. *Effect of process variables on permeation flux*

Among the dependent variables, permeate flux is the most sensitive response. This is because the permeate flux is affected by the operating pressure, the viscosity of feed solution, the osmotic pressure, the membrane resistance, the phenomenon of concentration polarization and the membrane fouling [8]. The susceptible characteristic of permeate flux explains the great deviation of the observed permeate flux in Table 2. The difference between the highest flux (13.88 $L.m^{-2}.h^{-1}$ in Run 7) and the lowest flux (3.65 $L.m^{-2}.h^{-1}$in Run 12) is as much as 73.70%.

In this study, a reduced quadratic model is used to represent the effect of process variables on the permeation flux. The final quadratic model contains only A, C, D, E, C^2, E^2 AE, BE and CE after further removal of insignificant terms. The ANOVA results of the reduced quadratic model are summarized in Table 6. The "lack of fit F-value" of 3.85 implies the phenomenon lack of fit is not important relative to the pure error; therefore, the final quadratic model is expected to fit the observed permeate flux well. Besides that, the final quadratic model possesses great R^2 of 0.9945. Thus, the chosen model is adequate to represent the observed permeate flux. The final quadratic model is also expected to explain new data well since the predicted R^2 achieves 0.9871 which is relatively high. Based on the number of terms in the final quadratic model, the value of adjusted R^2 is calculated at 0.9923. The difference of predicted R^2 and adjusted R^2 is less than 0.20, signifying that the model is adequate and outliers are absent.

Eqs. (6) and (7) are the equations for the permeate flux prediction using the final quadratic model in coded terms and actual terms respectively. The perturbation plot

(Fig. 7) shows that the temperature (factor A) and the pressure (factor E) give synergetic effect on the permeate flux. On the other hand, the feed concentration of salt (factor C) and the pH of feed solution (factor D) antagonistically affect the permeate flux. It is obvious that the permeate flux is mainly affected by the changes of pressure and temperature. The variation of the feed solution pH in the range 5 to 9 seems to give little effect on the permeate flux.

$$\text{Flux} = 6.81 + 2.22A - 0.54C - 0.12D + 2.30\times10^{-0.55}C^2 + 1.28E^2 + 0.77AE - 0.30CE \quad (6)$$

$$\text{Flux} = 10.01 - 0.00815\,(\text{temperature}) + 0.0739\,C_{\text{Nacl}} - 0.06186\,(\text{pH}) - 2.8795\,(\text{pressure}) - 6.2\times10^{-4}\,C_{\text{Nacl}}^{2} + 0.204715\,(\text{pressure})^2 + 0.024783\,(\text{temperature})\,(\text{pressure}) - 3.98\times10^{-3}\,(C_{\text{Nacl}})\,(\text{pressure}) \quad (7)$$

In this pressure driven process, it is reasonable to observe the greatest synergetic effect of pressure on the permeate flux. On the other hand, varying the pH of feed solutions results only in small changes of permeate flux. The increasing of permeate flux is possibly due to structure changes or thickness reduction of silica layer in more acidic solution [31]. Meanwhile, the dependence of permeate flux on solution temperature has been studied and reported by several previous researchers [25,27]. A possible explanation is that the dynamic viscosity of dye-salt-water mixture declines with elevated solution temperature. The reduction of dynamic viscosity promotes the diffusion rate through the membrane and results in the increment of permeate flux. The effect of temperature on the permeate flux also depends on the level of pressure as temperature increase in a pressurized separation cell. At higher salt concentration in the feed solutions, the permeate flux decreases significantly. The observation may be due to the growing resistance originating from concentration polarization [26]. Besides that, the opposing effect of interaction term (CE) on the permeate flux is possibly caused by osmotic pressure. Osmotic pressure is unavoidable in this design space as the concentration of salt in the feed solution is relatively high (20–80 g/L). The increment of salt concentration causes the rise of osmotic pressure so the effective pressure becomes lower [8]. The permeate flux is eventually reduced as the actual driving force becomes lesser. Consequently, the effect of pressure on the permeate flux depends on the salt concentration in the feed solutions.

Contour plots and surface response plots for the predicted permeate flux are illustrated in Figs. 8–10. All plots show the changes of the permeate flux based on the variation of two factors while other factors are held at midpoint level. It is observed that high permeate flux is achieved by operating membrane separation at high temperature and pressure. The addition of salt into the feed solution results in relatively low permeation which is undesirable. For the range of salt concentration 20–80 g/L, it is preferable to set the operating pressure to be higher than 7.5 bar. This is because existence of saddle point as shown in Fig. 9. An operating pressure lower than 7.5 bar will cause an extremely low permeate flux. From Fig. 10, adjusting pH to an acidic phase only promotes a small increment in permeate flux.

3.4. Optimization using a nonlinear programming method

It is always necessary to determine a set of operating conditions that in some sense all responses (dye retention, salt retention permeate flux) are optimized or at least kept in desired ranges. A popular approach is to formulate and solve the problem as a constrained optimization problem. The constraints for optimum operation conditions of dye-salt-water separation using the newly developed membrane have been summarized in Table 3. In general, NF membranes are used to decolorize the textile wastewater which mainly consists of salts and dyes. The highly

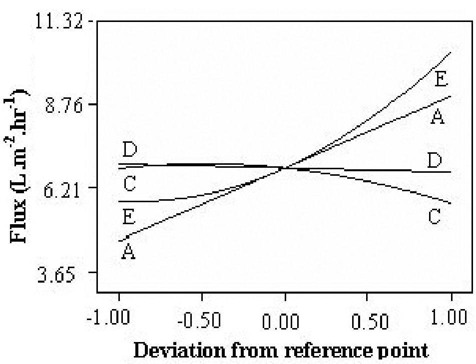

Fig. 7. Perturbation plot for permeate flux.

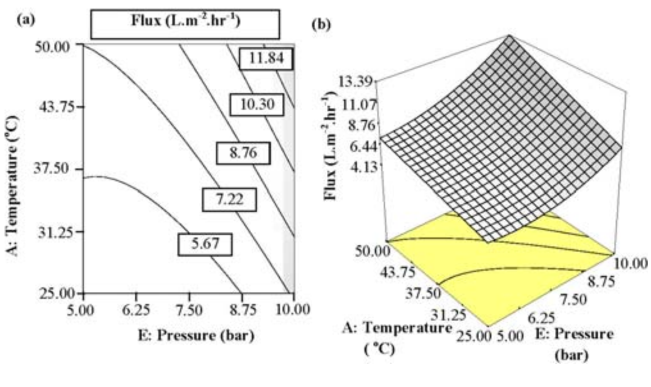

Fig. 8. (a) Contour plot and (b) surface response plot for effect of pressure and temperature on permeate flux ($C_{F,\text{NaCl}}$ = 50 g/L, pH =7, $C_{F,\text{dye}}$ = 2 g/L).

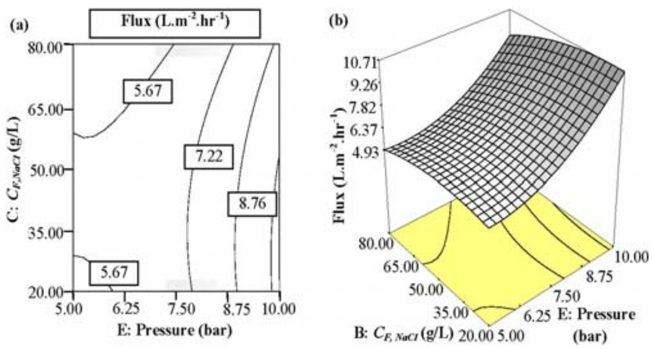

Fig. 9. (a) Contour plot and (b) surface response plot for effect of pressure and feed concentration of salt on permeate flux (temperature = 37.5°C, pH = 7, $C_{F,\text{dye}}$ = 2 g/L).

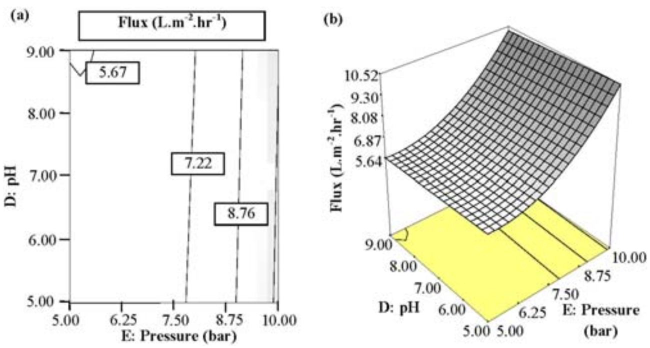

Fig. 10. (a) Contour plot and (b) surface response plot for effect of pressure and on pH on permeate flux (temperature = 37.5°C, $C_{F,\text{NaCl}}$ = 50 g/L, $C_{F,\text{dye}}$ = 2 g/L).

Table 7
Solutions for optimum operation conditions of dye–salt water separation using A025/Si

No.	T (°C)	$C_{F,\text{dye}}$ [a] (g/L)	$C_{F,\text{salt}}$ [b] (g/L)	pH	P (bar)	R_{dye} [c] (%)	R_{salt} [d] (%)	Flux (L.m^{-2}.h^{-1})	Desirability
1	50.0	2.94	80.00	5.0	10.0	98.01	26.15	12.12	0.7871
2	50.0	3.00	80.00	5.9	10.0	98.10	26.20	12.00	0.7837
3	50.0	2.94	80.00	5.0	10.0	97.98	26.38	12.02	0.7808
4	43.4	3.00	80.00	5.8	10.0	98.11	26.17	10.44	0.7173

[a]Feed concentration of dye; [b]Feed concentration of salt; [c]Rejection of dye; [d]Rejection of salt/

concentrated dye solution is later recycled back to the dyeing process to reduce the amount of wastewater. In addition, minimum salt rejection has to be achieved to maximize desalting. Thus, the constraints for this study are to achieve maximum dye separation, minimum salt separation and high permeate flux for the NF of dye-salt-water mixture. However, the importance of achieving dye retention is lower as the dye rejection is quite stable in the common operating conditions. The Design Expert software package calculates the desired solution by using a direct search procedure. The possible solutions are summarized in Table 7. Using the first solution in Table 7, the experiment (four replications) is carried out to verify the models generated previously. The average dye retention is 98.65% and the average salt retention is 25.76%. Meanwhile, the permeate flux is as high as 12.05 L.m^{-2}.h^{-1}. The experiment result shows that the predicted values are close to the experimental values with error less than 2%.

4. Conclusions

For a high desirability of maximum dye retention, minimum salt retention and maximum flux, the separation process has to be operated at high pressure and temperature. If the feed concentration of salt is low, a lower pressure is required to achieve a low salt retention. However, the permeate flux suffers a great reduction as the prediction flow rate is less than 10 L.m^{-2}.h^{-1}. In the future application of the bimodal porous silica/γ-alumina membrane, further improvement of permeate flux is highly desired.

In conclusion, the information is useful to guide engineers rapidly and efficiently along a path of improvement towards the general vicinity of the optimum conditions when a newly developed membrane is employed. Once the region of the optimum has been found, a more elaborate model, such as the extended Spiegler–Kedem model, may be employed to ensure further optimization of hydrodynamics conditions.

References

[1] I. Koyuncu and D. Topacik, Separ. Purif. Technol., 33(3) (2003) 283– 294.
[2] C. Allègre, P. Moulin, M. Maisseu and F. Charbit, J. Membr. Sci., 269(1–2) (2006) 15–34.
[3] G. Vishnu and K. Joseph, Color. Technol., 123(4) (2007) 260–266.
[4] C. Guizard and L. Cot, Membrane Science and Technology, Elsevier, Amsterdam, 1996.
[5] A. Erswell, C.J. Brouckaert and C.A. Buckley, Desalination, 70 (1988) 157–167.
[6] R. Jiraratananon, A. Sungpet and P. Luangsowan, Desalination, 130 (2000) 177–183.
[7] A. Akbari, J.C. Remigy and P. Aptel, Chem. Eng. Process., 41(7) (2002) 601–609.
[8] I. Koyuncu, D. Topacik and M.R. Wiesner, Water Res., 38(2) (2004) 432–440.
[9] A. Akbari, S. Desclaux, J.C. Rouch and J.C. Remigy, J. Membr. Sci., 297 (2007) 243–252.

[10] Z. Ji, Y. He and G. Zhang, Desalination, 201 (2006) 255–266.
[11] I. Petrinić, N.P.R. Andersen, S. Šostar-Turk and A.M. LeMarechal, Dyes Pigment., 74(3) (2007) 512–518.
[12] B. Van der Bruggen, E.Curcio and E. Drioli, J. Environ. Manage., 73(3) (2004) 267–274.
[13] L. Xu, W. Li, S. Lu, Z. Wang, Q. Zhu and Y. Ling, Desalination, 149 (2002) 199–203.
[14] I. Voigt, M. Stahn, S. Wohner, A. Junghans, J. Rost and W. Voigt, Sep. Purif. Technol., 25(1–3) (2001) 509–512.
[15] S.Y. Lee, S.J. Lee, S.J. Kwon, S.M. Yang and S.B. Park, J. Membr. Sci., 108(1–2) (1995) 97–105.
[16] J.H. So, S.M. Yang and S.B. Park, J. Membr. Sci., 147(2) (1999) 147–158.
[17] C.Y. Tsai, S.Y. Tam, Y.F. Lu and C.J. Brinker, J. Membr. Sci., 169(2) (2000) 255–268.
[18] Y. Yoshino, T. Suzuki, B.N. Nair, H. Taguchi and N. Itoh, J. Membr. Sci., 267(1–2) (2005) 8–17.
[19] A.L. Ahmad, C.P. Leo and S.R. Abd. Shukor, J. Am. Ceram. Soc., 91(6) (2008) 2009–2014.
[20] D.C. Montgomery, Design of Experiment, Wiley, New York, 2001.
[21] A.L. Ahmad, C.P. Leo and S.R. Abd. Shukor, Thin Solid Films, 516(12) (2008) 4319–4324.
[22] A.L. Ahmad, C.P. Leo and S.R. Abd. Shukor, J. Am. Ceram. Soc., 91(1) (2008) 246–251.
[23] C.K. Lambert and R.D. Gonzalex, Mater. Lett., 38(2) (1999) 145–149.
[24] I. Honma, H.S. Zhou, D. Kundu and A. Endo, Adv. Mater., 12(10) (2000) 1529–1533.
[25] I. Koyuncu, D. Topacik and E. Yuksel, Separ. Purif. Technol., 36(1) (2004) 77–85.
[26] M. Al-Aseeri, Q. Bu-Ali, S. Haji and N. Al-Bastaki, Desalination, 206 (2007) 407–413.
[27] Y. Ku, P.L. Lee and W.Y. Wang, J. Membr. Sci., 250(1–2) (2005) 159–165.
[28] M. Mulder, Basic Principles of Membrane Technology, Kluwer Academic, Dordrecht, 1996.
[29] C. Bellona, J.E. Drewes, P. Xu and G. Amy, Water Res., 38(12) (2004) 2795–2809.
[30] W.R. Bowen and A.W. Mohammad, Desalination, 117 (1998) 257–264.
[31] A. Doyle and B.K. Hodnett, Micropor. Mesoporous Mater., 63(1–3) (2003) 53–57.